This article has been accepted for publication in a future issue of this journal, but has not been fully edited. Content may change prior to final publication. Citation information: DOI 10.1109/TMC.2019.2895034, IEEE Transactions on Mobile Computing

Hidden-node Problem in Full-duplex Enabled CSMA Networks

Shengbo Liu, Liqun Fu, *Senior Member, IEEE*, and Wei Xie

Abstract—The in-band full-duplexing is a promising technique to boost wireless network throughput by allowing a node to transmit and receive simultaneously. This paper provides a comprehensive investigation on the hidden-node problem that arises in the full-duplex (FD) enabled CSMA (carrier-sensing multiple-access) networks. In particular, we first provide the fundamental conditions that guarantee successful receptions for all the FD transmission cases, and propose an ellipse interference model and an ellipse carrier-sensing model to capture the interference relation and the carrier-sensing mechanism in FD CSMA networks, respectively. We further establish the hidden-node-free design in FD CSMA networks. Specifically, we show the sufficient conditions on the carrier-sensing power threshold that can eliminate hidden-node collisions. We show that compared with half-duplex CSMA networks, the FD CSMA network needs a much smaller carrier-sensing power threshold to prevent hidden-node collisions, which leads to poor network spatial reuse. This motivates us to further propose a new MAC protocol with Full-duplex Enhanced Carrier-Sensing (FECS) mechanism. The FECS-MAC enables the secondary carrier-sensing before starting the secondary transmission. We show that with the secondary carrier-sensing design, the required carrier-sensing power threshold can be increased while keeping the network hidden-node free. Therefore, the network spatial reuse and throughput can be significantly improved. Simulation results demonstrate that the FECS-MAC can improve the throughput of dense three-node FD networks by more than 30%, compared with relay full-duplex (RFD) MAC protocol proposed in [1].

Index Terms—Hidden-node problem, CSMA, full-duplex, carrier-sensing

1 Introduction

The in-band full-duplex (FD) capability, that allows a node to transmit and receive simultaneously in the same frequency band, is a promising technique to boost the capacity of wireless networks [2], [3]. It has been demonstrated that with two antennas at the receiver, the self-interference can be canceled to the noise level [4], [5]. Thus, ideally, FD technology can double the link rate of a single pair of nodes by enabling bi-directional transmissions. To fully exploit the FD gain in a general wireless network, the medium access control (MAC) protocol needs to be carefully designed.

The carrier-sense multiple-access with collision avoidance (CSMA/CA), such as IEEE 802.11, is the most widely used MAC protocol in distributed wireless networks. In recent years, many research efforts have been put on modifying the CSMA/CA protocol stacks to adapt the FD transmissions [3], [6], [7]. A critical problem in the half-duplex (HD) CSMA networks is the hidden-node problem [8]. If it is not solved properly, it may cause the degradation of the network throughput due to heavy collisions [9]. Therefore, a natural question to ask is: is hidden-node collision still a critical problem in the FD CSMA networks?

It is widely believed that the FD technology can alleviate (if not completely solve) the hidden-node problem in CSMA networks [2], [10]. The main argument is that with full-duplexing, a receiver can immediately start a transmission or send a busy tone to suppress the nodes around the receiver starting concurrent transmissions. However, through rigorous analysis, we are reaching a contrary conclusion: the hidden-node problem in FD CSMA networks is not alleviated, but even more severe than the one in the HD CSMA networks. The key reason behind this finding is that with FD transceivers, there are more transmission cases which cause different interference patterns. For example, full-duplexing not only can enable bi-directional transmissions between two nodes, but also can enable two separate transmissions between one node and two other different nodes. The latter transmission case is important because it can enable simultaneous uplink and downlink transmissions between an access point (AP) and two different clients in the infrastructure based networks, or create cut-through routing in a multi-hop wireless network [11]. However, it involves three nodes in the transmissions, which causes a more complicated interference footprint. This sets a more stringent requirement on the carrier-sensing mechanism to prevent hidden-node collisions. Therefore, it is of great importance to establish a rigorous hidden-node-free design in the FD CSMA networks.

Within this context, this paper provides a comprehensive study on the hidden-node problem in FD CSMA networks. We first consider all the possible FD transmission cases and provide a formal definition of hidden-node problem by finding all the conditions that may cause hidden-node collisions. Furthermore, in order to give a rigorous analysis, simple and accurate models are needed to capture the interference relations and the carrier-sensing relations among FD links. Most of the studies on HD CSMA networks adopt the interference range and the carrier-sensing range based models [8], [12]. However, we find that such range concept based interference and carrier-sensing models are

- *Shengbo Liu and Liqun Fu are with the School of Information and Science Technology, and with the Key laboratory of Underwater Acoustic Communication and Marine Information Technology Ministry of Education, Xiamen University, Xiamen, China. Email: liqun@xmu.edu.cn*
- *Wei Xie is with Nokia, Shanghai, China. Email: weixie.ee@gmail.com*

This article has been accepted for publication in a future issue of this journal, but has not been fully edited. Content may change prior to final publication. Citation information: DOI 10.1109/TMC.2019.2895034, IEEE Transactions on Mobile Computing

not applicable to FD CSMA networks, because each FD transmission always has two concurrent active nodes. The power radiation of two currently active nodes cannot be modeled by a single distance. Therefore, we propose the ellipse interference model and ellipse carrier-sensing model to capture the interference relation and the carrier-sensing mechanism in FD CSMA networks, respectively. These two ellipse models may be useful in many other theoretical works on the FD CSMA networks, not just the hidden-node-free design here.

Next, we establish the FD hidden-node-free design. Specifically, we show a sufficient condition on the carrier-sensing power threshold which guarantees that the hidden-node collisions can be eliminated in FD CSMA networks. Notice that this result works for any network topology, because we do not make any assumption on the link distribution. We find that the carrier-sensing power threshold to prevent collisions in FD CSMA networks needs to be set much smaller than the one in HD CSMA networks. The main reason is that the three-node FD transmissions expand two ellipse interference regions. Thus, although FD technology may double the link throughput of each FD transmission, the FD gain in a general FD CSMA network might be much smaller because of the worse spatial reuse.

Given the above results, the next issue is can we further improve the spatial reuse (and thus the network throughput) of the FD CSMA network while keeping it hidden-node-free? This motivates us to propose a new MAC protocol with the Full-duplex Enhanced Carrier-Sensing (FECS) mechanism. The FECS-MAC is also compatible with HD transmission. The key idea in FECS-MAC is that it enables secondary carrier-sensing before starting the secondary transmission on the three-node FD link-pair. With this design, while keeping the network hidden-node-free, it can pack concurrent FD transmission link-pairs in a tighter way, and thus improve the spatial reuse. Furthermore, the secondary carrier-sensing can also suppress the inter-node interference on the same three-node FD link-pair. Simulation results show that the FECS-MAC can improve the throughput of two-node FD networks by more than 100%, compared with the half-duplex CSMA MAC protocol, and improve the throughput of dense three-node FD networks by more than 30%, compared with the relay full-duplex (RFD) MAC protocol proposed in [1].

1.1 Related Work

In the literature, most studies on the hidden-node-free design focus on the half-duplex CSMA networks [8], [13], [14]. Physical carrier-sensing (PCS) and RTS/CTS handshaking, which is also called "virtual carrier-sensing" are two main techniques to combat the hidden-node collisions. Xu et al. [8] showed that hidden nodes can be eliminated if the carrier-sensing range is set larger than the transmission range plus the interference range. However, Jiang et al. [13] proved that such carrier-sensing range setting is not large enough to eliminate hidden nodes, and they further proposed to use non-uniform carrier-sensing to remove hidden nodes and reduce exposed nodes. Haas and Deng [14] devised a new MAC protocol termed dual busy tone multiple access to solve hidden-node and exposed-node problems completely. However, the range based interference models and carrier-sensing models used in [8], [13], [14], cannot be applied to FD CSMA networks.

There are only few papers that discussed about the hidden-node problem in FD CSMA networks. It is believed in [3], [4], [15], that the FD technology can solve the hidden-node problem as the receiver also serves as a transmitter. Reference [16] showed that hidden-node problem still exists in the bi-directional transmissions due to asymmetric data packets, and such collision can be prevented by sending busy tone signals. However, the studies in [3], [4], [15], [16] only consider the hidden-node problem in the bi-directional transmissions with full-duplexing. Ref. [9] showed that the hidden-node collisions may arise in the three-node FD transmissions. Ref. [17] focused on the throughput analysis of an FD CSMA network with one access point (AP) and several clients. The authors in [17] introduced an additional collision notification signal sent out by the AP once the hidden-node collision occurs. However, both [9] and [17] did not provide rigorous analysis and effective solutions to prevent the hidden-node collisions from happening.

Recently, the MAC protocol design to enable FD transmissions has attracted a lot of research attention [1], [3], [6], [7], [9], [18], [19]. Ref. [7] presented a centralized FD MAC protocol, which controls the rate and time of transmission to maximize the network throughput. Distributed FD MAC protocols based on random access were proposed in [3], [6], [9], [19]. Specifically, ref. [9] considered the two-node FD transmissions, and ref. [3] considered the three-node destination-based FD transmissions, respectively. Ref. [19] proposed a two-node FD protocol and studied the effects of spatial reuse and asynchronous contention on the FD capacity gain. The MAC protocol proposed in [6] covers all the FD transmission cases. The MAC protocols proposed in [18], [20] are based on RTS/CTS handshaking. However, none of these protocols focus on the hidden-node-free design. Our FECS-MAC protocol not only supports all the FD transmission cases, but also prevents hidden-node collisions effectively.

The rest of this paper is organized as follows. In Section II, we present the system model, and propose the ellipse interference model and the ellipse carrier-sensing model. Section III shows the full-duplex hidden-node-free design. In Section IV, we introduce the FECS-MAC protocol. Section V presents the simulation results, and Section VI concludes this paper.

2 SYSTEM MODEL

We consider an FD CSMA network, which is composed of a set of FD link pairs $\mathcal{L} = \{l_i, 1 \leq i \leq |\mathcal{L}|\}$. The FD CSMA network is general. It can be either an ad-hoc network or a WLAN (wireless local area network), where APs (access points) serve multiple users. With in-band full-duplex capability, when a receiver is receiving packets, it can transmit to its transmitter or another node at the same time on the same frequency band. Thus, each FD link pair l_i has three possible transmission cases, as shown in Fig. 1:

1) Two-node FD transmission: The transmitter T_i does carrier sensing and captures the channel. It transmits to its receiver R_i, and R_i also has packets for T_i.

This article has been accepted for publication in a future issue of this journal, but has not been fully edited. Content may change prior to final publication. Citation information: DOI 10.1109/TMC.2019.2895034, IEEE Transactions on Mobile Computing

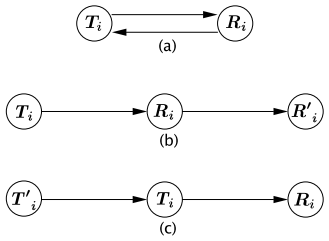

Fig. 1. Three FD transmission cases.

In this case, there exist bi-directional transmissions between T_i and R_i, as shown in Fig. 1(a). The link pair in this FD transmission is denoted by $l_i(T_i, R_i)$.

2) Three-node destination-based FD transmission: The transmitter T_i does carrier sensing and captures the channel. It starts a primary transmission to its receiver R_i, and R_i has packets for a third node R'_i. Thus, R_i initiates a secondary transmission to R'_i, as shown in Fig. 1(b). The link pair in this FD transmission is denoted by $l_i(T_i, R_i, R'_i)$.
3) Three-node source-based FD transmission: The transmitter T_i does carrier sensing and captures the channel. It starts a primary transmission to its receiver R_i. Meanwhile, a third node T'_i has packets for T_i, and initiates a secondary transmission to T_i, as shown in Fig. 1(c). The link pair in this FD transmission is denoted by $l_i(T'_i, T_i, R_i)$.

2.1 Transmission Model

We assume that all nodes in the network use the same transmit power P_t, which cannot be arbitrarily large. The radio signal propagation follows the log-distance path model with path loss exponent $2 < \alpha < 6$ [13]. The path-gain from T_i to R_i is

$$G(T_i, R_i) = G_0 d(T_i, R_i)^{-\alpha},$$

where $d(T_i, R_i)$ is the Euclidean distance between T_i and R_i, and G_0 is the reference path gain at the reference distance of 1 meter. Let d_{max} denote $\max_i d(T_i, R_i)$, which is the maximum link length in the network. A node decodes its signal successfully if and only if the received Signal-to-Interference-plus-Noise Ratio (SINR) is above a certain threshold.

In CSMA networks, a successful packet transmission requires that both the DATA frame and the ACK frame are received correctly. Consider two FD link pairs l_i and l_j. We assume that l_i is not interfered by l_j if all the DATA and ACK frames of both the FD transmissions on l_i are received successfully. We assume that the interfering signal is treated as noise at the receiver.

Notice that the SINR conditions of successful transmissions for two-node FD link pair and three-node FD link pair are different. When l_i is a two-node FD link pair, it is not interfered by l_j if both the following conditions are satisfied:

$$\frac{P_t G(T_i, R_i)}{P_t G(S_j, R_i) + P_t G(S'_j, R_i) + I_{SI} + n_0} \geq \gamma_0, \quad (1)$$

$$\frac{P_t G(R_i, T_i)}{P_t G(S_j, T_i) + P_t G(S'_j, T_i) + I_{SI} + n_0} \geq \gamma_0, \quad (2)$$

where I_{SI} is the self-interference, n_0 is the background noise, and S_j , S'_j represent the two transmitters on l_j, respectively. We assume that all nodes in the network adopt the same SINR threshold γ_0. The interference consists of the interference from l_j and self-interference.

When l_i is a three-node destination-based FD link pair, it is not interfered by l_j if the following four conditions are satisfied:

$$\frac{P_t G(T_i, R_i)}{P_t G(S_j, R_i) + P_t G(S'_j, R_i) + I_{SI} + n_0} \geq \gamma_0, \quad \text{(DATA to } R_i\text{)}, \quad (3)$$

$$\frac{P_t G(R_i, R'_i)}{P_t G(S_j, R'_i) + P_t G(S'_j, R'_i) + P_t G(T_i, R'_i) + n_0} \geq \gamma_0, \text{(DATA to } R'_i\text{)}, \quad (4)$$

$$\frac{P_t G(R'_i, R_i)}{P_t G(S_j, R_i) + P_t G(S'_j, R_i) + I_{SI} + n_0} \geq \gamma_0, \quad \text{(ACK to } R_i\text{)}, \quad (5)$$

$$\frac{P_t G(R_i, T_i)}{P_t G(S_j, T_i) + P_t G(S'_j, T_i) + P_t G(R'_i, T_i) + n_0} \geq \gamma_0, \text{(ACK to } T_i\text{)}. \quad (6)$$

Notice that the interference consists of the interference from l_j and self-interference in conditions (3) and (5). However, in conditions (4) and (6), the interference consists of the interference from l_j and the inter-node interference on the same link.

Similarly, when l_i is a three-node source-based FD transmission link pair, it is not interfered by l_j if the following four conditions are satisfied:

$$\frac{P_t G(T_i, R_i)}{P_t G(S_j, R_i) + P_t G(S'_j, R_i) + P_t G(T'_i, R_i) + n_0} \geq \gamma_0, \text{(DATA to } R_i\text{)}, \quad (7)$$

$$\frac{P_t G(T'_i, T_i)}{P_t G(S_j, T_i) + P_t G(S'_j, T_i) + I_{SI} + n_0} \geq \gamma_0, \quad \text{(DATA to } T_i\text{)}, \quad (8)$$

$$\frac{P_t G(R_i, T_i)}{P_t G(S_j, T_i) + P_t G(S'_j, T_i) + I_{SI} + n_0} \geq \gamma_0, \quad \text{(ACK to } T_i\text{)}, \quad (9)$$

$$\frac{P_t G(T_i, T'_i)}{P_t G(S_j, T'_i) + P_t G(S'_j, T'_i) + P_t G(R_i, T'_i) + n_0} \geq \gamma_0, \text{(ACK to } T'_i\text{)}. \quad (10)$$

If l_i is not interfered by l_j, and l_j is not interfered by l_i, l_i and l_j do not interfere with each other, and can be active simultaneously.

Definition 1 (interference feasible set)**.** *Let $\mathcal{S}^{IF} \subseteq \mathcal{L}$ denote a subset of link pairs. If for any two link pairs l_i and $l_j \in \mathcal{S}^{IF}$, they do not interfere with each other, set $\mathcal{S}^{IF}$ is then called interference feasible set such that all the simultaneous transmissions on the link pairs in $\mathcal{S}^{IF}$ are successful.*

2.2 Ellipse Interference Model

In half-duplex networks, usually an interference range is defined to model whether two links interfere with each other or not [12]. Such interference range concept is not applicable to FD networks, because there are always two simultaneously active transmitters on any link pair. Thus, we propose the ellipse interference model to capture the interference relation among FD link pairs.

This article has been accepted for publication in a future issue of this journal, but has not been fully edited. Content may change prior to final publication. Citation information: DOI 10.1109/TMC.2019.2895034, IEEE Transactions on Mobile Computing

Ellipse interference model: Consider two active transmitters S_j and S'_j. We use an ellipse with S_j and S'_j as its focuses to model the interference region. Let $2c$ denote its focal length where $c = \frac{1}{2}d(S_j, S'_j)$. Consider a receiver N_i with a tolerable interference level I_i^{tol} from another link pair in the network. Let E_{IR_i} denote the semi-major axis of the interference ellipse. The value of E_{IR_i} can be derived from the following equation[1]:

$$P_t G_0 (E_{IR_i} - c)^{-\alpha} + P_t G_0 (E_{IR_i} + c)^{-\alpha} = I_i^{tol}. \quad (11)$$

Receiver N_i is not interfered by the active nodes S_j and S'_j as long as it is outside the ellipse, i.e.,

$$d(S_j, N_i) + d(S'_j, N_i) > 2E_{IR_i}. \quad (12)$$

The following proposition shows the accuracy of the ellipse interference model:

Proposition 1. *Consider any receiver N_i, if it satisfies condition* (12) *in the ellipse interference model, it is not interfered by the transmissions of S_j and S'_j , i.e., its received interference power from S_j and S'_j is below its tolerable interference level I_i^{tol}.*

Proof. We first show that if N_i locates on the ellipse, its received interference power from S_j and S'_j at most is I_i^{tol}. Let x denotes $d(S_j, N_i)$. When N_i is on the ellipse, its received interference power from S_j and S'_j is:

$$I_{N_i} = P_t G_0 x^{-\alpha} + P_t G_0 (2E_{IR_i} - x)^{-\alpha}, E_{IR_i} - c \le x \le E_{IR_i} + c.$$

By symmetry, it is sufficient to consider the range $E_{IR_i} - c \le x \le E_{IR_i}$. The first order derivative of I_{N_i} with respect to x is

$$\frac{dI_{N_i}}{dx} = P_t G_0 \alpha \left((2E_{IR_i} - x)^{-\alpha - 1} - x^{-\alpha - 1} \right).$$

We can find that when $E_{IR_i} - c \le x \le E_{IR_i}$, $\frac{dI_{N_i}}{dx} \le 0$. Thus, I_{N_i} is a decreasing function of x. When $x = E_{IR_i} - c$, I_{N_i} reaches it maximum value. Then we have

$$I_{N_i} \le P_t G_0 (E_{IR_i} - c)^{-\alpha} + P_t G_0 (E_{IR_i} + c)^{-\alpha} = I_i^{tol}.$$

Therefore, if N_i is outside the ellipse, it received power is below I_i^{tol}. □

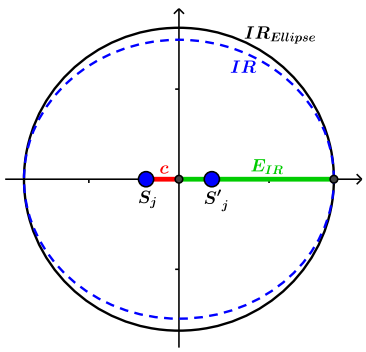

Fig. 2. Ellipse model of interference region.

Fig. 2 shows the geometric interpretation of the ellipse interference model. Given the tolerable interference level I_i^{tol}, the dotted curve represents the real interference region, i.e., the total interference power from S_j and S'_j on the dotted curve is equal to I_i^{tol}. The solid curve shows the ellipse interference region. When $c = \frac{1}{2}d_{max}$, $\alpha = 4$, and I_i^{tol} varies from 0.05 to 0.2 with the step size of 0.01, the average ratio of the area of the real interference region to the area of the ellipse interference region is 89.81%. It illustrates that the ellipse interference model is quite accurate in modeling the interference relation for FD transmissions.

The tolerable interference level I_i^{tol} is related to the SINR requirements (1)-(10). In particular, in order to satisfy conditions (1), (2), (3), (5), (8), and (9), I_i^{tol} can be set as follows:

$$I_i^{tol} = \frac{P_t G_0 d_{max}^{-\alpha}}{\gamma_0} - I_{SI} - n_0. \quad (13)$$

In order to satisfy conditions (4), (6), (7), and (10), I_i^{tol} can be set as follows:

$$I_i^{tol} = \frac{P_t G_0 d_{max}^{-\alpha}}{\gamma_0} - I_{IN} - n_0, \quad (14)$$

where I_{IN} is the inter-node interference on the same link-pair.

It has been shown that the self-interference I_{SI} can be reduced to the noise level [2]. However, in the three-node FD transmission, it is difficult to cancel the inter-node interference I_{IN} at the receiver [9]. From condition (14), we know that large inter-node interference leads to small tolerable interference level, which makes E_{IR} quite large according to equation (11). This means that, if the inter-node interference is large, the separation of two concurrently active three-node FD link pairs need to be increased. As a result, the network spatial reuse is reduced. Therefore, before establishing the secondary transmission in a three-node FD link, the inter-node interference should be limited below a certain threshold:

$$I_{IN} \le \frac{1}{K} P_t G_0 d_{max}^{-\alpha}, \quad (K \ge \gamma_0). \quad (15)$$

The control parameter K should be set much larger than γ_0 to suppress the inter-node interference. Since I_{IN} is usually much larger than I_{SI}, the tolerable interference level I^{tol} of three-node FD link-pair is smaller than that of two-node FD link-pair. So the ellipse interference region $IR_{Ellipse}$ in three-node FD link-pair is much larger. What's more, if the interfering link-pair l_j is a three-node FD link-pair, the concurrent active transmitters S_j and S'_j for DATA frames are different from the transmitters for ACK frames. Consequently, there are two ellipse interference regions with different focuses for a three-node FD link-pair.

2.3 Ellipse Carrier-sensing Model

In CSMA networks, carrier sensing is designed to prevent collisions. Ideally, it should avoid the violation of (1) - (10). In the current CSMA based FD protocols [3], [6], the carrier-sensing is done by the initiating transmitter T_i. We consider the carrier sensing by energy detection. If T_i senses a power $P^{CS}(T_i)$ greater than a power threshold P_{th}, i.e.,

$$P^{CS}(T_i) > P_{th},$$

it will not transmit, and its back-off countdown process will be frozen.

1. Notice that it is difficult to find a closed-form expression of E_{IR_i} from (11). The value of E_{IR_i} can be found efficiently through solving (11) by typical methods, such as bi-section search.

This article has been accepted for publication in a future issue of this journal, but has not been fully edited. Content may change prior to final publication. Citation information: DOI 10.1109/TMC.2019.2895034, IEEE Transactions on Mobile Computing

The carrier sensing range concept is introduced in most studies of HD CSMA networks [12], [21]. If two transmitters T_i and T_j are outside the carrier-sensing range, T_i and T_j cannot carrier sense each other. However, in FD CSMA networks, the carrier-sensed power by T_i consists of the total power of two simultaneously active transmitters on another link-pair. Thus, the carrier-sensing range cannot be applied to FD CSMA networks. Therefore, we propose the ellipse carrier-sensing model to capture the carrier-sensing mechanism in FD CSMA networks.

Ellipse carrier-sensing model: Consider two link-pairs l_i and l_j. We use an ellipse with its focuses as the two active transmitters S_j and S'_j to model the carrier-sensing region, termed as $CSR_{Ellipse}$. Let c and E_{CS} denote the focal length and the semi-major axis of $CSR_{Ellipse}$, respectively. The value of c is $\frac{1}{2}d(S_j, S'_j)$. Given the carrier-sensing power threshold P_{th}, the value of E_{CS} is given by:

$$E_{CS} = \left(\frac{P_{th}}{2P_tG_0}\right)^{-\frac{1}{\alpha}}.$$

If transmitter T_i is inside the $CSR_{Ellipse}$, i.e.,

$$d(T_i, S_j) + d(T_i, S'_j) < 2E_{CS}, \tag{16}$$

transmitter T_i will sense the transmissions of S_j and S'_j. Thus it will not transmit, and its back-off countdown process will be frozen.

The following proposition shows the accuracy of the ellipse carrier-sensing model:

Proposition 2. *If T_i satisfies condition* (16)*, its carrier-sensed power caused by the transmissions of S_j and S'_j is larger than the carrier-sensing power threshold P_{th}.*

Proof. We first show that if T_i locates on the $CSR_{Ellipse}$, its carrier-sensed power caused by S_j and S'_j at least is P_{th}. Let $x = d(T_i, S_j)$. When T_i is on the $CSR_{Ellipse}$, its received carrier-sensed power is:

$$P^{CS}(T_i) = P_tG_0x^{-\alpha} + P_tG_0(2E_{CS} - x)^{-\alpha},$$

where $E_{CS} - c \le x \le E_{CS} + c$. By symmetry, it is sufficient to consider the range $E_{CS} - c \le x \le E_{CS}$. Following the same method as in the proof on Proposition 1, we can show that $P^{CS}(T_i)$ is a decreasing function of x, when $E_{CS} - c \le x \le E_{CS}$. Thus, when $x = E_{CS}$, $P^{CS}(T_i)$ reaches it minimum value, i.e.,

$$P^{CS}(T_i) \ge 2P_tG_0E_{CS}^{-\alpha} = P_{th}.$$

This means that if T_i locates on the $CSR_{Ellipse}$, its carrier-sensed power caused by S_j and S'_j is no less than P_{th}. Furthermore, we can find that if T_i is inside $CSR_{Ellipse}$, its carrier-sensed power is larger than P_{th}. □

Fig. 3 shows the geometric interpretation of the ellipse carrier-sensing model. The solid curve is the ellipse carrier-sensing region $CSR_{Ellipse}$. The dotted curve represents the real carrier-sensing region, i.e., the total carrier-sensed power of a transmitter on the dotted curve is equal to P_{th}. We can find that the $CSR_{Ellipse}$ is inside the dotted curve. When $c = \frac{1}{2}d_{max}$, $\alpha = 4$, and E_{CS} varies from $3d_{max}$ to $5d_{max}$ with the step size of $0.1d_{max}$, the average ratio of the area of the ellipse carrier-sensing region to the area of the real carrier-sensing region is 96.08%. This shows that the ellipse carrier-sensing model is an appropriate model in modeling the carrier-sensing mechanism in FD CSMA networks.

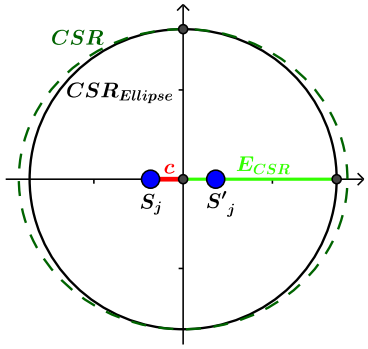

Fig. 3. Ellipse model of carrier-sensing region.

Choosing an appropriate P_{th}, (and the corresponding E_{CS} in the $CSR_{Ellipse}$) is crucial to the performance of a FD CSMA network. On one hand, it needs to guarantee that conditions (1) - (10) are satisfied in order to prevent hidden-node collisions. On the other hand, If P_{th} is set too small, which means that the E_{CS} is too large, it will reduce the spatial reuse and the network throughput unnecessarily.

3 Hidden-node-free Design

In this section, we first show that compared with half-duplex transmission, the hidden-node problem could be more severe in FD CSMA networks. Furthermore, we derive a sufficient condition for the carrier-sensing power threshold P_{th} (and the corresponding E_{CS} of the carrier-sensing ellipse) that can eliminate hidden-node collisions for FD CSMA networks.

We focus on the distributed random access mode in IEEE 802.11 protocol [22]. In the default operation in most 802.11 products, when a receiver has already sensed a signal from another node in the network, it will not attempt to receive a later signal from its own transmitter, even if the later signal is stronger. This is called the "Receiver-Capture effect", which may cause transmission failure [23]. Such transmission failure cannot be prevented with the carrier-sensing mechanism [24]. Fortunately, it can be solved with the receiver "RS (Restart) Mode". With RS mode, a receiver will switch to receive the stronger signal if its SINR condition can be satisfied. When discussing the hidden-node-free design, it is required that the "RS Mode" is enabled at the receiver [24].

3.1 Hidden-node Problem in FD CSMA Networks

It has been shown in [12] that in HD CSMA networks, the hidden-node collisions can be eliminated by setting carrier-sensing power threshold as:

$$P_{th} = P_tG_0\left(\left(\gamma_0^{\frac{1}{\alpha}} + 2\right)d_{max}\right)^{-\alpha}. \tag{17}$$

In the following, we use an example network shown in Fig. 4 to illustrate that the hidden-node problem is more severe

This article has been accepted for publication in a future issue of this journal, but has not been fully edited. Content may change prior to final publication. Citation information: DOI 10.1109/TMC.2019.2895034, IEEE Transactions on Mobile Computing

in FD CSMA networks, i.e., even P_{th} is set according to (17), hidden-node collisions may still occur.

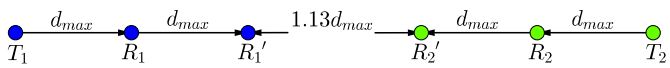

Fig. 4. Hidden-node in three-node FD network.

Figure 4 shows two three-node FD transmission link-pairs $l_1(T_1, R_1, R_1')$ and $l_2(T_2, R_2, R_2')$. The distances among the nodes are $d(T_1, R_1) = d(R_1, R_1') = d(T_2, R_2) = d(R_2, R_2') = d_{max}$, and $d(R_1', R_2') = 1.13d_{max}$. The SIR requirement $\gamma_0 = 10$, and the path-loss exponent $\alpha = 4$. According to (17), P_{th} is equal to $P_t G_0 \left(3.78 d_{max}\right)^{-4}$.

Suppose that T_2 wants to initiate a transmission while T_1 and R_1 are sending packets to R_1 and R_1', respectively. Transmitter T_2 senses a power $P^{CS}(T_2)$ given by

$$\begin{aligned} P^{CS}(T_2) &= P_t G_0 (5.13 d_{max})^{-4} + P_t G_0 (4.13 d_{max})^{-4} \\ &= P_t G_0 (3.783 d_{max})^{-4} < P_{th}. \end{aligned}$$

Thus, T_2 senses the channel to be idle and initiates FD transmissions on link-pair l_2. After T_1 and R_1 finishes DATA frames transmissions, R_1 and R_1' need to return ACK frames to T_1 and R_1, respectively. Then the SIR at R_2' is

$$\begin{aligned} &\frac{P_t G_0 d_{max}^{-4}}{P_t G_0 \left((1.13 d_{max})^{-4} + (2.13 d_{max})^{-4} + (2 d_{max})^{-4}\right)} \\ &= 1.38 < \gamma_0. \end{aligned}$$

Thus, collision happens at R_2' due to insufficient SIR. Notice that if we consider the inter-node interference on link-pair $l_2(T_2, R_2, R_2')$, the SIR will be further reduced. Therefore, the carrier-sensing power threshold P_{th} that can prevent hidden-node collisions in HD CSMA networks is not sufficient to prevent hidden-node collisions in FD CSMA networks. FD CSMA networks need a more stringent setting on P_{th} to prevent hidden-node collisions.

3.2 Hidden-node-free Design in FD CSMA Networks

Since different FD transmission cases have different interference footprint, we provide the sufficient conditions on P_{th} to prevent hidden-node collisions for the two-node FD transmissions and three-node FD transmissions, respectively, as shown in Theorem 1 and Theorem 2.

Theorem 1. *It is sufficient to prevent hidden-node collisions in two-node FD CSMA networks, if the semi-major axis of the carrier-sensing ellipse is set as*

$$E_{CS} = E_{IR2} + d_{max}, \tag{18}$$

equivalently, if the carrier-sensing power threshold is set as

$$P_{th} = 2 P_t G_0 (E_{IR2} + d_{max})^{-\alpha}, \tag{19}$$

where E_{IR2} is derived from the following equation:

$$(E_{IR2} - \frac{d_{max}}{2})^{-\alpha} + (E_{IR2} + \frac{d_{max}}{2})^{-\alpha} = \frac{d_{max}^{-\alpha}}{\gamma_0} - \frac{I_{SI} + n_0}{P_t G_0}. \tag{20}$$

Proof. Without loss of generality, suppose $l_i(T_i, R_i)$ starts transmissions first. Its currently active transmitters are T_i and R_i (sending DATA or ACK). If $l_j(T_j, R_j)$ can start concurrent transmissions with l_i, according to Proposition 2, we know that T_j is outside the $CSR_{Ellipse}(T_i, R_i)$. Thus we have:

$$d(T_i, T_j) + d(R_i, T_j) > 2(E_{IR2} + d_{max}). \tag{21}$$

Next we show that if inequality (21) is satisfied, l_i and l_j do not interfere with each other. Using the triangular inequality, we have

$$\begin{aligned} &d(T_i, T_j) + d(R_i, T_j) \\ &\le d(T_i, R_j) + d(R_j, T_j) + d(R_i, R_j) + d(R_j, T_j) \\ &\le 2 d_{max} + d(T_i, R_j) + d(R_i, R_j). \end{aligned} \tag{22}$$

According to (21) and (22), we have

$$d(T_i, R_j) + d(R_i, R_j) > 2 E_{IR2}. \tag{23}$$

Thus, from (21) and (23), we know that both T_j and R_j on link-pair l_j are outside the ellipse interference region centered at T_i and R_i. Furthermore, because E_{IR2} satisfies equation (20), according to Proposition 1, we know that T_j and R_j can tolerate an interference level of $\frac{P_t G_0}{\gamma_0} d_{max}^{-\alpha} - I_{SI} - n_0$, which is sufficient to ensure that the SINRs at T_j and R_j are all greater than γ_0. Therefore, we know that l_j is not interfered by l_i.

We further prove that l_i is not interfered by l_j either. Using the triangular inequality, we have

$$\begin{aligned} d(T_i, T_j) + d(R_i, T_j) &\le d(T_i, T_j) + d(T_i, T_j) + d(T_i, R_i) \\ &\le 2 d(T_i, T_j) + d_{max}. \end{aligned} \tag{24}$$

According to (21) and (24), we have

$$d(T_i, T_j) > E_{IR2} + 0.5 d_{max}. \tag{25}$$

Similarly, we can also have

$$d(R_i, T_j) > E_{IR2} + 0.5 d_{max}. \tag{26}$$

Furthermore, consider inequality (23). Using the same method, we have

$$d(T_i, R_j) > E_{IR2} - 0.5 d_{max}, \tag{27}$$

$$d(R_i, R_j) > E_{IR2} - 0.5 d_{max}. \tag{28}$$

Thus, from inequalities (25), (26), (27) and (28), we can find that

$$\begin{aligned} d(T_i, T_j) + d(T_i, R_j) &> 2 E_{IR2}, \\ d(R_i, T_j) + d(R_i, R_j) &> 2 E_{IR2}. \end{aligned}$$

This means that both T_i and R_i are outside the ellipse interference region of l_j. Thus, according to Proposition 1, we know that l_i is not interfered by l_j either. Therefore, condition (19) is sufficient to guarantee the successful transmissions on both l_i and l_j. □

Theorem 2. *It is sufficient to prevent hidden-node collisions in three-node FD CSMA networks, if the semi-major axis of the carrier-sensing ellipse is set as*

$$E_{CS} = E_{IR3} + 3 d_{max}, \tag{29}$$

equivalently, if the carrier-sensing power threshold is set as

$$P_{th} = 2 P_t G_0 (E_{IR3} + 3 d_{max})^{-\alpha}, \tag{30}$$

This article has been accepted for publication in a future issue of this journal, but has not been fully edited. Content may change prior to final publication. Citation information: DOI 10.1109/TMC.2019.2895034, IEEE Transactions on Mobile Computing

where E_{IR3} is derived from the following equation:

$$(E_{IR3}-\frac{d_{max}}{2})^{-\alpha}+(E_{IR3}+\frac{d_{max}}{2})^{-\alpha}=\left(\frac{1}{\gamma_0}-\frac{1}{K}\right)d_{max}^{-\alpha}-\frac{n_0}{P_tG_0}. \quad (31)$$

Proof. We consider the worst-case three-node FD CSMA networks that consist of three-node destination-based FD link-pairs. For a three-node destination-based FD link-pair, the concurrent active transmitters for DATA frames are different from the transmitters for ACK frames. Thus, there are two ellipse interference regions with different focuses.

Without loss of generality, suppose $l_i(T_i, R_i, R_i')$ starts transmissions first. Its concurrent active transmitters can be T_i and R_i (sending DATA), or R_i and R_i' (sending ACK). If $l_j(T_j, R_j, R_j')$ can start concurrent transmissions with $l_i(T_i, R_i, R_i')$, transmitter T_j needs to ensure that its carrier-sensed power is below the power threshold given in (30). The carrier-sensed power can be from nodes T_i and R_i, or nodes R_i and R_i'. According to Proposition 2, we know that T_j is outside the $CSR_{Ellipse}(T_i, R_i)$ or $CSR_{Ellipse}(R_i, R_i')$. This means that at least one of the following two inequalities is satisfied:

$$d(T_i,T_j)+d(R_i,T_j)>2(E_{IR3}+3d_{max}), \quad \text{or} \quad (32)$$
$$d(R_i,T_j)+d(R_i',T_j)>2(E_{IR3}+3d_{max}). \quad (33)$$

Let us first show that if inequality (32) is satisfied, l_i and l_j do not interfere with each other. Using the triangular inequality, we have

$$\begin{aligned}&d(T_i,T_j)+d(R_i,T_j)\\&\le d(T_i,R_j)+d(R_j,T_j)+d(R_i,R_j)+d(R_j,T_j)\\&\le 2d_{max}+d(T_i,R_j)+d(R_i,R_j) \quad (34)\\&\le 2d_{max}+d(T_i,R_j')+d(R_i,R_j')+2d(R_j',R_j)\\&\le 4d_{max}+d(T_i,R_j')+d(R_i,R_j'). \quad (35)\end{aligned}$$

According to (32),(34), and (35), we have

$$d(T_i,R_j)+d(R_i,R_j)>2E_{IR3}+4d_{max}, \quad (36)$$
$$d(T_i,R_j')+d(R_i,R_j')>2E_{IR3}+2d_{max}. \quad (37)$$

Thus, from (32), (36), and (37), we know that all the three nodes T_j, R_j, and R_j' on link-pair l_j are outside the ellipse interference region centered at T_i and R_i.

Similarly, using triangular inequality, we also have

$$\begin{aligned}&d(T_i,T_j)+d(R_i,T_j)\\&\le d(T_i,R_i)+d(R_i,T_j)+d(R_i,R_i')+d(R_i',T_j)\\&\le 2d_{max}+d(R_i,T_j)+d(R_i',T_j) \quad (38)\\&\le 2d_{max}+d(R_i,R_j)+d(R_i',R_j)+2d(R_j,T_j)\\&\le 4d_{max}+d(R_i,R_j)+d(R_i',R_j) \quad (39)\\&\le 4d_{max}+d(R_i,R_j')+d(R_i',R_j')+2d(R_j',R_j)\\&\le 6d_{max}+d(R_i,R_j')+d(R_i',R_j'). \quad (40)\end{aligned}$$

According to (32), (38), (39), and (40), we have

$$d(R_i,T_j)+d(R_i',T_j)>2E_{IR3}+4d_{max}, \quad (41)$$
$$d(R_i,R_j)+d(R_i',R_j)>2E_{IR3}+2d_{max}, \quad (42)$$
$$d(R_i,R_j')+d(R_i',R_j')>2E_{IR3}. \quad (43)$$

This means that all the three nodes T_j, R_j, and R_j' on link-pair l_j are outside the ellipse interference region centered at R_i and R_i'. Thus, T_j, R_j, and R_j' are outside both the ellipse interference regions of l_i. Furthermore, because E_{IR3} satisfies equation (31), according to Proposition 1, we know that T_j, R_j, and R_j' can tolerate an interference level of $P_tG_0\left(\frac{1}{\gamma_0}-\frac{1}{K}\right)d_{max}^{-\alpha}-n_0$, which is sufficient to ensure that the SINRs at T_j, R_j, and R_j' are all greater than γ_0. Therefore, we know that l_j is not interfered by l_i.

Next we prove that if inequality (32) is satisfied, l_i is not interfered by l_j either. Using the triangular inequality, we have

$$\begin{aligned}d(T_i,T_j)+d(R_i,T_j)&\le d(T_i,T_j)+d(T_i,T_j)+d(T_i,R_i)\\&\le 2d(T_i,T_j)+d_{max}. \quad (44)\end{aligned}$$

Combing (32) and (44), we have

$$d(T_i,T_j)>E_{IR3}+2.5d_{max}. \quad (45)$$

Similarly, we can also show that

$$d(R_i,T_j)>E_{IR3}+2.5d_{max}. \quad (46)$$

Furthermore, consider inequalities (36), (37), (41), (42), and (43). Using the same method, we have

$$d(T_i,R_j)>E_{IR3}+1.5d_{max}, d(R_i,R_j)>E_{IR3}+1.5d_{max}, \quad (47)$$
$$d(T_i,R_j')>E_{IR3}+0.5d_{max}, d(R_i,R_j')>E_{IR3}+0.5d_{max}, \quad (48)$$
$$d(R_i,T_j)>E_{IR3}+1.5d_{max}, d(R_i',T_j)>E_{IR3}+1.5d_{max}, \quad (49)$$
$$d(R_i,R_j)>E_{IR3}+0.5d_{max}, d(R_i',R_j)>E_{IR3}+0.5d_{max}, \quad (50)$$
$$d(R_i,R_j')>E_{IR3}-0.5d_{max}, d(R_i',R_j')>E_{IR3}-0.5d_{max}. \quad (51)$$

Thus, from inequalities (45), (46), (47), (48), (49), (50), and (51), we can find that

$$\begin{aligned}&d(R_i',R_j)+d(R_i',R_j')>2E_{IR3},\\&d(R_i,R_j)+d(R_i,R_j')>2E_{IR3},\\&d(T_i,R_j)+d(T_i,R_j')>2E_{IR3}+2d_{max},\\&d(R_i',T_j)+d(R_i',R_j)>2E_{IR3}+2d_{max},\\&d(R_i,T_j)+d(R_i,R_j)>2E_{IR3}+4d_{max},\\&d(T_i,T_j)+d(T_i,R_j)>2E_{IR3}+4d_{max}.\end{aligned}$$

This means that all the three nodes T_i, R_i and R_i' are outside both the ellipse interference regions of l_j. Therefore, l_i is not interfered by l_j. Following the same method, we can show that if inequality (33) is satisfied, l_i and l_j do not interfere with each other. Therefore, condition (30) is sufficient to guarantee the successful transmissions on l_i and l_j. □

Notice that since we do not impose any assumption on the link distribution, the carrier-sensing power thresholds provided in Theorem 1 and Theorem 2 can guarantee interference-free transmissions for FD CSMA networks with any topology. The required P_{th} values (or the corresponding E_{CS} values of the carrier-sensing ellipse) are mainly dependent on the maximum link distance d_{max}, the path loss exponent α, the self-interference I_{SI}, and the inter-node interference parameter K. Since I_{SI} is much smaller than the inter-node interference, from equations (20) and

This article has been accepted for publication in a future issue of this journal, but has not been fully edited. Content may change prior to final publication. Citation information: DOI 10.1109/TMC.2019.2895034, IEEE Transactions on Mobile Computing

TABLE 1
Carrier Sensing Threshold Comparison

	E_{CS}	P_{th}
Two-node FD networks	$3.35d_{max}$	$P_tG_0(2.82d_{max})^{-4}$
Three-node FD networks	$6.23d_{max}$	$P_tG_0(5.35d_{max})^{-4}$
HD networks	—	$P_tG_0(3.78d_{max})^{-4}$

(31), we can find that the required E_{IR3} is larger than E_{IR2}. Furthermore, from equations (18) and (29), we can find that the required E_{CS} for three-node FD links is much larger than that of two-node FD links. The main reason is that the three-node FD transmissions expand two ellipse interference regions. Therefore, the required P_{th} to prevent hidden-node collisions in three-node FD CSMA networks is smaller than that of two-node FD CSMA networks. In a FD CSMA network that is composed of both the two-node and three-node FD links, it needs to adopt the required carrier-sensing power threshold in three-node FD CSMA network (as shown in (30)) to eliminate hidden-node collisions.

Let us further compare the required P_{th} to prevent hidden-node collisions in FD CSMA networks with the one in HD CSMA networks, as shown in (17). Table 1 shows the corresponding E_{CS} and P_{th} for HD and FD CSMA networks, when $\gamma_0 = 10$, $\alpha = 4$, $K = 13$, $d_{max} = 50m$, $n_0 = -90dbm$, and $I_{SI} = -90dbm$, which are typical values for wireless communication. We can find that if the FD CSMA network only consists of two-node FD links, the required P_{th} is larger than the one in HD CSMA networks. This means that the two-node FD transmissions can alleviate the hidden-node problem. Furthermore, we can observe that the E_{CS} of a three-node FD link is much larger than that of a two-node FD link. In a general FD network which is composed of HD links, two-node FD links, and three-node FD links, the P_{th} needs to be set to $P_tG_0(5.35d_{max})^{-4}$ to avoid hidden-node problem. Compared with HD networks, the P_{th} needs to be reduced by a factor of 3.7. A smaller P_{th} implies a larger E_{CS} of the carrier-sensing ellipse. As a result, the spatial reuse in FD CSMA networks is reduced. Therefore, although the FD technology may double the link throughput of each FD link, the FD gain of a general FD CSMA network might be much smaller because of the worse spatial reuse.

4 FD MAC Protocol Design

In order to improve the spatial reuse of FD CSMA network while keeping it hidden-node-free, we design a new distributed MAC protocol with Full-duplex Enhanced Carrier-Sensing (FECS) based on the CSMA/CA. The FECS-MAC supports all FD transmission cases. Furthermore, in order to avoid inter-node interference in a three-node FD transmission, the Power-Exchange (PE) algorithm is used to collect potential information of inter-node interference before establishing the secondary transmission. The key idea in FECS-MAC is that it enables both the primary and secondary transmitters of a FD transmission link to do carrier-sensing. Therefore, the required P_{th} to prevent hidden-node collisions can be set much larger.

4.1 Power Set

In a three-node FD transmission, it is required that the inter-node interference on the same link-pair is smaller than a certain value, i.e., it needs to satisfy Condition (15). Thus, we adopt the Power Exchange (PE) algorithm in [12] to construct the "power set".

In the PE algorithm, each node periodically broadcasts special Power-Exchange (PE) packets and receives PE packets from neighbor nodes with the minimum physical rate. The PE packets are used for information exchange, which contain one type of information: "power set". The transmit power for PE packets is the same as that for regular packets, and all nodes have the same receive sensitivity. The PE algorithm consists two steps:

1) Each node a measures the received power of PE packets transmitted by any other node c, and stores the power information in a "power set" $\mathcal{P}_a = \{P(a,c)\}$. Note that $P(a,c) = P(c,a)$ by reciprocity.
2) Each node periodically broadcasts a PE packet that contains its power set to nearby nodes with the minimum physical rate.

Actually, PE packets need to be sent only when the network conditions or topology have changed. Periodically broadcasting PE packet is aimed to enhance the robustness of the PE algorithm. With the power sets, the secondary transmitter of the three-node FD link can ensure that Condition (15) is satisfied before starting the secondary transmission. In particular, for the case of three-node destination-based FD transmission, R_i needs to check R_i' (or T_i)'s power set to make sure that the inter-node interference, which is the received power of R_i' from T_i, satisfies Condition (15). For the case of three-node source-based FD transmission, T_i' needs to check its (or R_i's) power set to ensure that the inter-node interference, which is the received power of R_i from T_i', satisfies Condition (15).

4.2 FECS Mechanism

In the existing FD MAC protocols, only the primary transmitter does carrier-sensing. An FD transceiver at least has two antennas and two active RF chains [25]. Thus, except the FD transmission duration, a node can use one antenna and one RF chain to transmit (or receive) signal, and use the other antenna and RF chain to perform carrier-sensing [26]. This enables the secondary transmitter in the three-node FD link to perform carrier-sensing to determine whether the channel status permits to establish the secondary transmission. Thus, in the three-node destination-based FD link shown in Fig. 1(b), before R_i starts the secondary transmission, it needs to ensure that its detected power subtracted by the received power of the primary transmission is below a power threshold P_{th}^D, i.e.,

$$P^{CS}(R_i) - P(T_i, R_i) < P_{th}^D, \tag{52}$$

where $P(T_i, R_i)$ can be obtained from power sets of R_i.

In the three-node source-based FD link shown in Fig. 1(c), before T_i' starts the secondary transmission, it needs to ensure that its detected power subtracted by its received power from T_i is below a power threshold P_{th}^S, i.e.,

$$P^{CS}(T_i') - P(T_i, T_i') < P_{th}^S, \tag{53}$$

This article has been accepted for publication in a future issue of this journal, but has not been fully edited. Content may change prior to final publication. Citation information: DOI 10.1109/TMC.2019.2895034, IEEE Transactions on Mobile Computing

where $P(T_i, R_i)$ can be obtained from power sets of T_i'.

Next, we describe the protocol in each FD transmission case.

4.3 Two-node FD Transmission

Figure 5 shows the two-node FD transmission between T_i and R_i. Node T_i captures the channel and successfully initiates the primary transmission to R_i. Node R_i waits for a SIFS time during which it can receive and decode the MAC header from T_i. [2] If R_i has a packet for T_i, it starts sending a DATA frame to T_i, which creates a two-node FD transmission. If R_i has a packet for another node, this belongs to the three-node destination-based transmission case which is to be discussed later. If R_i has no packet to send, it does nothing. After R_i starts transmitting, both T_i and R_i receive a packet and compare the packet durations. The node that finishes transmission earlier will continue to send a busy-tone signal to ensure that the two DATA transmissions end at the same time. After the DATA frame transmissions, T_i and R_i wait for a SIFS time, and then send ACKs simultaneously.

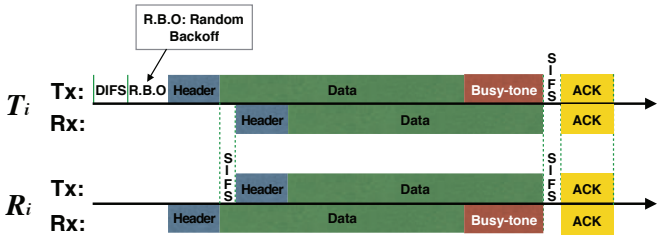

Fig. 5. Two-node FD transmission

4.4 Three-node Destination-based FD Transmission

Figure 6 shows the three-node destination-based FD transmission. Node T_i captures the channel and successfully initiates the primary transmission to R_i. After receiving the MAC header and waiting for a SIFS time, R_i does not have a packet for T_i. Instead, it has a packet for R_i'. Node R_i sends a packet to R_i', if both the following conditions are satisfied:

1) the secondary carrier-sensed power at R_i satisfies Condition (52),
2) the inter-node interference satisfies Condition (15);

otherwise R_i does nothing. If P_{th}^D in (52) is set small enough, the first condition ensures that the transmission of R_i will not interfere other links. The second condition can ensure that the packet from R_i can be successfully decoded at R_i' without being interfered by the primary transmission. After R_i starts transmitting a DATA frame to R_i', actually, both T_i and R_i' will receive the packet from R_i. Therefore, both T_i and R_i can compare the DATA frame durations. The node that finishes earlier will continue to send a busy-tone signal to ensure that the two DATA transmissions end at the same time. After the DATA frame transmissions, R_i and R_i' wait for a SIFS time, and then send ACKs at the same time.

2. Here we assume that MAC header can be decoded during packet reception, which have been verified in [3], [4], [17], [27].

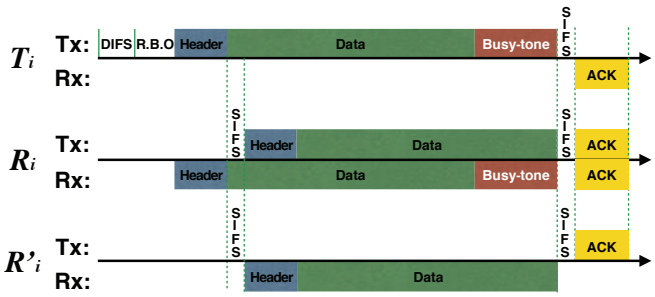

Fig. 6. Destination-based three-node FD transmission

4.5 Three-node Source-based FD Transmission

Figure 7 shows the three-node source-based FD transmission. Node T_i captures the channel and successfully initiates the primary transmission to R_i. After receiving the MAC header, R_i does not have any packet to send, but some other nodes may have packets for T_i. When R_i is decoding the MAC header from T_i, other nodes that have packets for T_i can also decode this MAC header and know the received power from T_i. After receiving the MAC header, all the nodes that have packets for T_i first wait for a DIFS time, and then compete the opportunity to send packets to T_i through the random back-off mechanism. The following three conditions need to be satisfied before T_i' starts the secondary transmission to T_i:

1) the secondary carrier-sensed power at T_i' satisfies Condition (53) during the DIFS time and the back-off countdown process;
2) the inter-node interference satisfies Condition (15);
3) the countdown process of T_i' ends first.

Notice that the power threshold P_{th}^S needs to be small enough to ensure that if R_i has started transmitting packets, Condition (53) will not hold. Thus, it can prevent the transmission of T' if R_i has started transmissions. The second condition makes sure that R_i can successfully receive the packet from T_i without being interfered by the transmission from T_i'. Furthermore, once the countdown process of T_i' ends first, other nodes that have packets for T_i will detect the transmission of T_i'. Thus, they will freeze their countdown processes due to the violation of Condition (53). After T_i' starts transmitting DATA frame to T_i, both T_i and T_i' compare the DATA frame durations. The node that finishes earlier sends a busy-tone until the other node finishes its DATA frame. Then after a SIFS time, T_i and R_i reply ACKs simultaneously.

By performing the secondary carrier-sensing, the power thresholds in the FECS-MAC that can prevent hidden-node collisions can be significantly increased, as shown in the following theorem.

Theorem 3. *In FECS-MAC, it is sufficient to prevent hidden-node collisions in three-node FD CSMA networks, if the primary carrier-sensing power threshold P_{th}, and the secondary carrier-*

This article has been accepted for publication in a future issue of this journal, but has not been fully edited. Content may change prior to final publication. Citation information: DOI 10.1109/TMC.2019.2895034, IEEE Transactions on Mobile Computing

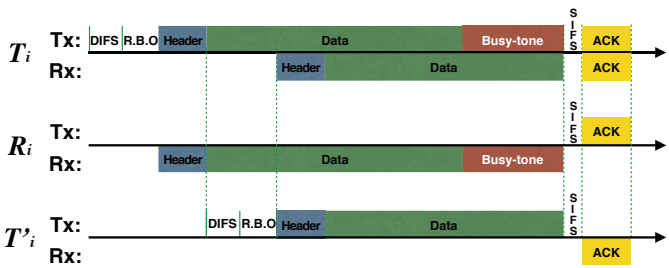

Fig. 7. Source-based three-node FD transmission

sensing power thresholds P_{th}^D and P_{th}^S are set as

$$P_{th} = 2P_tG_0(E_{IR3} + 2d_{max})^{-\alpha}, \quad (54)$$
$$P_{th}^D = 2P_tG_0(E_{IR3} + 2d_{max})^{-\alpha}, \quad (55)$$
$$P_{th}^S = P_tG_0(2d_{max})^{-\alpha}, \quad (56)$$

where E_{IR3} is derived from Equation (31).

Proof. Consider two three-node FD link-pairs l_i and l_j. Without loss of generality, suppose l_i starts transmission first. It can be a destination-based three-node FD link-pair or a source-based three-node FD link-pair. When l_i is a destination-based three-node FD link-pair, we will prove that Conditions (54) and (55) together ensure no mutual interference between l_i and l_j if l_j is a destination-based three-node FD link-pair; and Conditions (54) and (56) together ensure no mutual interference between l_i and l_j if l_j is a source-based three-node FD link-pair.

When l_j is a destination-based three-node FD link-pair, from (54), we know that at least one of the following two inequalities is satisfied:

$$d(T_i, T_j) + d(R_i, T_j) > 2(E_{IR3} + 2d_{max}), \quad \text{or} \quad (57)$$
$$d(T_i', T_j) + d(T_i, T_j) > 2(E_{IR3} + 2d_{max}). \quad (58)$$

If (57) is satisfied, using the triangular inequality, we have

$$d(T_i, T_j) + d(R_i, T_j) \le d(T_i, R_i') + d(R_i', T_j) + d(R_i, T_j) \le 2d_{max} + d(R_i', T_j) + d(R_i, T_j). \quad (59)$$

Combining (57) and (59), we have

$$d(R_i, T_j) + d(R_i', T_j) > 2E_{IR3} + 2d_{max}. \quad (60)$$

From (55), we know that

$$d(T_i, R_j) + d(R_i, R_j) > 2(E_{IR3} + 2d_{max}). \quad (61)$$

Using the triangular inequality, we have

$$d(T_i, R_j) + d(R_i, R_j) \le d(T_i, R_i') + d(R_i', R_j) + d(R_i, R_j) \le 2d_{max} + d(R_i', R_j) + d(R_i, R_j). \quad (62)$$

Combining (61) and (62), we have

$$d(R_i, R_j) + d(R_i', R_j) > 2E_{IR3} + 2d_{max}. \quad (63)$$

Using the triangular inequality, we have

$$d(T_i, R_j) + d(R_i, R_j) \le 2d(R_j, R_i') + d(T_i, R_j') + d(R_i, R_j') \le 2d_{max} + d(T_i, R_j') + d(R_i, R_j'). \quad (64)$$

Combining (61) and (64), we have

$$d(T_i, R_j') + d(R_i, R_j') > 2E_{IR3} + 2d_{max}. \quad (65)$$

Using the triangular inequality, we have

$$d(T_i, R_j') + d(R_i, R_j') \le d(T_i, R_i') + d(R_i, R_j') + d(R_i', R_j') \le 2d_{max} + d(R_i, R_j') + d(R_i', R_j'). \quad (66)$$

Combining (65) and (66), we have

$$d(R_i, R_j') + d(R_i', R_j') > 2E_{IR3}. \quad (67)$$

According to (57), (60), (61), (63), (65), and (67), we know that T_j, R_j and R_j' are outside both the ellipse interference regions of l_i. Thus, l_j is not interfered by l_i. Next we prove that l_i is not interfered by l_j either. Consider inequality (57). Using the triangular inequality, we have

$$d(T_i, T_j) + d(R_i, T_j) \le d(T_i, T_j) + d(T_i, T_j) + d(T_i, R_i) \le 2d(T_i, T_j) + d_{max}. \quad (68)$$

Combing (57) and (68), we have

$$d(T_i, T_j) > E_{IR3} + 1.5d_{max}. \quad (69)$$

Similarly, we can also show that

$$d(R_i, T_j) > E_{IR3} + 1.5d_{max}. \quad (70)$$

Furthermore, consider inequalities (60), (61), (63), (65) and (67). Using the same method, we have

$$d(T_i, R_j) > E_{IR3} + 1.5d_{max}, d(R_i, R_j) > E_{IR3} + 1.5d_{max}, \quad (71)$$
$$d(T_i, R_j') > E_{IR3} + 0.5d_{max}, d(R_i, R_j') > E_{IR3} + 0.5d_{max}, \quad (72)$$
$$d(R_i', T_j) > E_{IR3} + 0.5d_{max}, d(R_i', R_j) > E_{IR3} + 0.5d_{max}, \quad (73)$$
$$d(R_i', R_j') > E_{IR3} - 0.5d_{max}. \quad (74)$$

Thus, from inequalities (69)-(74), we can find that

$$\begin{aligned} &d(R_i', R_j) + d(R_i', R_j') > 2E_{IR3}, \\ &d(R_i, R_j) + d(R_i, R_j') > 2E_{IR3}, \\ &d(T_i, R_j) + d(T_i, R_j') > 2E_{IR3} + 2d_{max}, \\ &d(R_i', T_j) + d(R_i', R_j) > 2E_{IR3} + d_{max}, \\ &d(R_i, T_j) + d(R_i, R_j) > 2E_{IR3} + 2d_{max}, \\ &d(T_i, T_j) + d(T_i, R_j) > 2E_{IR3} + 3d_{max}. \end{aligned}$$

This means that T_i, R_i and R_i' are outside both the ellipse interference regions of l_j. Thus, l_i is not interfered by l_j. Following the same method, we can show that if inequality (58) is satisfied, l_i and l_j do not interfere with each other.

Next, we prove that when l_j is a source-based three-node FD link-pair, Conditions (54) and (56) together ensure no mutual interference between l_i and l_j. Condition (56) is used to ensure that T_j' and R_j won't start the secondary transmissions simultaneously. Given Condition (54), we know that inequality (57) or inequality (58) is satisfied. If (57) is satisfied, using the triangular inequality, we have

$$\begin{aligned} &d(T_i, T_j) + d(R_i, T_j) \\ &\le d(T_i, T_j') + d(T_j', T_j) + d(R_i, T_j') + d(T_j', T_j) \\ &\le 2d_{max} + d(T_i, T_j') + d(R_i, T_j'). \end{aligned} \quad (75)$$

This article has been accepted for publication in a future issue of this journal, but has not been fully edited. Content may change prior to final publication. Citation information: DOI 10.1109/TMC.2019.2895034, IEEE Transactions on Mobile Computing

Combining (57) and (75), we have

$$d(T_i, T_j') + d(R_i, T_j') > 2E_{IR3} + 2d_{max}. \quad (76)$$

Using the triangular inequality, we have

$$\begin{aligned} & d(T_i, T_j') + d(R_i, T_j') \quad (77) \\ & \leq d(T_i, R_i') + d(R_i', T_j') + d(R_i, T_j') \\ & \leq 2d_{max} + d(R_i', T_j') + d(R_i, T_j'). \quad (78) \end{aligned}$$

Combining (76) and (78), we have

$$d(R_i, T_j') + d(R_i', T_j') > 2E_{IR3}. \quad (79)$$

Using the triangular inequality, we have

$$\begin{aligned} & d(T_i, T_j) + d(R_i, T_j) \\ & \leq d(T_i, R_j) + d(R_j, T_j) + d(R_i, R_j) + d(R_j, T_j) \\ & \leq 2d_{max} + d(T_i, R_j) + d(R_i, R_j). \quad (80) \end{aligned}$$

Combining (57) and (80), we have

$$d(T_i, R_j) + d(R_i, R_j) > 2E_{IR3} + 2d_{max}. \quad (81)$$

Previously, we have shown that given (57), inequality (60) is satisfied. Using the triangular inequality, we have

$$\begin{aligned} & d(R_i, T_j) + d(R_i', T_j) \\ & \leq d(R_i, R_j) + d(R_j, T_j) + d(R_i', R_j) + d(R_j, T_j) \\ & \leq 2d_{max} + d(R_i, R_j) + d(R_i', R_j). \quad (82) \end{aligned}$$

Combining (60) and (82), we have

$$d(R_i, R_j) + d(R_i', R_j) > 2E_{IR3}. \quad (83)$$

Thus, from (57), (60), (76), (79), (81), and (83), we know that T_j, R_j and T_j' are outside both the ellipse interference regions of l_i. Thus, l_j is not interfered by l_i. Next we prove that l_i is not interfered by l_j either. Consider inequality (57). Using the triangular inequality, we have

$$\begin{aligned} d(T_i, T_j) + d(R_i, T_j) &\leq d(T_i, T_j) + d(T_i, R_i) + d(T_i, T_j), \\ &\leq 2d(T_i, T_j) + d_{max}. \quad (84) \end{aligned}$$

Combining (57) and (84), we have

$$d(T_i, T_j) > E_{IR3} + 1.5d_{max}. \quad (85)$$

Similarly, we have

$$d(R_i, T_j) > E_{IR3} + 1.5d_{max}. \quad (86)$$

With the same method, from inequalities (76), (81), (60), (79), and (83), we have

$$d(T_i, T_j') > E_{IR3} + 0.5d_{max}, d(R_i, T_j') > E_{IR3} + 0.5d_{max}, \quad (87)$$

$$d(T_i, R_j) > E_{IR3} + 0.5d_{max}, d(R_i, R_j) > E_{IR3} + 0.5d_{max}, \quad (88)$$

$$d(R_i', T_j) > E_{IR3} + 0.5d_{max}, d(R_i', T_j') > E_{IR3} - 0.5d_{max}, \quad (89)$$

$$d(R_i', R_j) > E_{IR3} - 0.5d_{max}. \quad (90)$$

Furthermore, from inequalities (85) - (90), we have

$$\begin{aligned} d(T_i, T_j) + d(T_i, R_j) &> 2E_{IR3} + 2d_{max}, \\ d(R_i, T_j) + d(R_i, R_j) &> 2E_{IR3} + 2d_{max}, \\ d(R_i', T_j) + d(R_i', R_j) &> 2E_{IR3}, \\ d(T_i, T_j) + d(T_i, T_j') &> 2E_{IR3} + 2d_{max}, \\ d(R_i, T_j) + d(R_i, T_j') &> 2E_{IR3} + 2d_{max}, \\ d(R_i', T_j) + d(R_i', T_j') &> 2E_{IR3}. \end{aligned}$$

This means that T_i, R_i and R_i' are outside both the ellipse interference regions of l_j. Thus, l_i is not interfered by l_j either. Following the same method, we can also show that if inequality (58) is satisfied, l_i and l_j do not interfere with each other.

When l_i is a source-based three-node FD link-pair, the proof is the same as the case when l_i is a destination-based three node FD link pair, and thus is omitted here. Therefore, Conditions (54), (55), and (56) are sufficient to prevent hidden-node collisions in three-node FD CSMA networks. □

We can find that the primary carrier sensing power threshold in equation (54) is still smaller than the required power threshold in the two-node FD CSMA networks, as shown in Theorem 1. Thus, in a general FD CSMA network that is composed of both the two-node and three-node FD links, the conditions in Theorem 3 are still sufficient to guarantee hidden-node-free transmissions. If without secondary carrier-sensing, the primary transmitter needs to guarantee the successful transmissions on both the primary and the secondary transmissions. In FECS-MAC, the primary transmitter only needs to ensure that the primary transmission is successful. By enabling the secondary carrier-sensing, the secondary transmitter only needs to guarantee the success of the secondary transmission. Thus the required carrier-sensing power thresholds in the FECS-MAC can be increased, which leads to a significant improvement of the spatial reuse and the network throughput.

5 SIMULATION RESULTS

We carry out extensive simulations with ns-3 network simulator [28] to verify the proposed hidden-node-free design (Theorems 1-3), and evaluate the performance of the proposed FECS-MAC. The two-ray ground propagation model is used with the system parameters shown in Table 2. We assume that during simulations all the nodes in the network have already known the power sets of their neighbor nodes.

TABLE 2
Simulation Parameters

Parameter	Value	Parameter	Value
SIFS	$16\mu s$	α	4
DIFS	$34\mu s$	γ_0	10
Data rate	$12Mpbs$	d_{max}	$50m$
$CW_{\min}$	31	P_t	$20mw$
Slot	$9\mu s$	Packet size	$1500bytes$

In the simulations, we consider the following three MAC protocols:

This article has been accepted for publication in a future issue of this journal, but has not been fully edited. Content may change prior to final publication. Citation information: DOI 10.1109/TMC.2019.2895034, IEEE Transactions on Mobile Computing

1) FECS: our proposed FD MAC with the primary and secondary carrier sensing.
2) HFD: the half-duplex CSMA MAC protocol, i.e., IEEE 802.11a.
3) RFD: the Relay Full-Duplex (RFD) MAC protocol proposed in [1].

5.1 Verification of the hidden-node-free Design

We investigate the collision rate of the network with two-node FD link-pairs shown in Fig. 8 (a), under different carrier-sensing power thresholds. The distance between R_1' and R_2' is d_{max}. Given the system parameters, Table 3 shows the carrier-sensing power thresholds calculated according to Theorems 1-3 and the ratios of the received power to the carrier-sensing power thresholds.

TABLE 3
CS Power Thresholds

Theorem	1	2	3
P_{th}	$-72.96dBm$	$-83.73dBm$	$-80.68dBm$
P_r/P_{th}	$18dB$	$29.1dB$	$23.1dB$

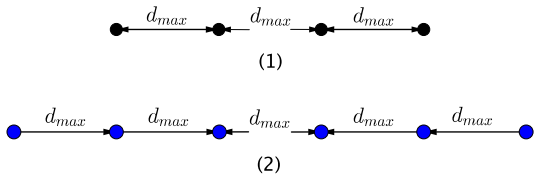

(a) An FD CSMA network with two FD link-pairs.

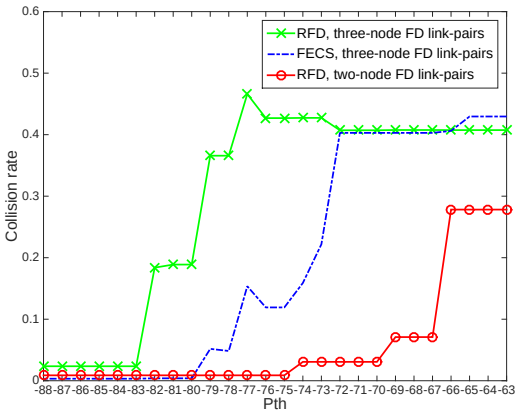

(b) Collision rate with different P_{th}.

Fig. 8. Verification of the hidden-node-free design.

Fig. 8 (b) shows the network collision rate as a function of the carrier-sensing power threshold. We can observe that if the carrier-sensing power thresholds are below the values given in Table 3, the collision rates are all reduced to very small values, i.e., below 3%. Furthermore, we find that with the help of secondary carrier-sensing, the power threshold in our proposed FECS-MAC to eliminate hidden-node collisions is increased from $-83.73dBm$ to $-80.68dBm$. Notice that the remaining collisions are because that in CSMA networks two transmitters may count down to zero simultaneously during the back-off process. Such collisions

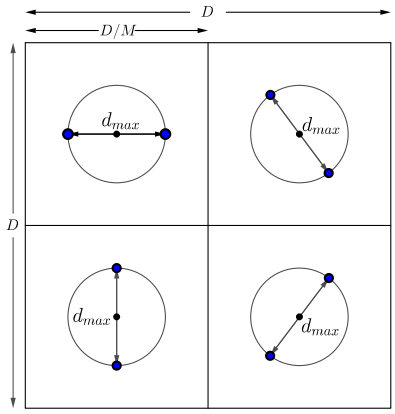

(a) Topology of a two-node FD network with $D = 800m$ and $M = 2$.

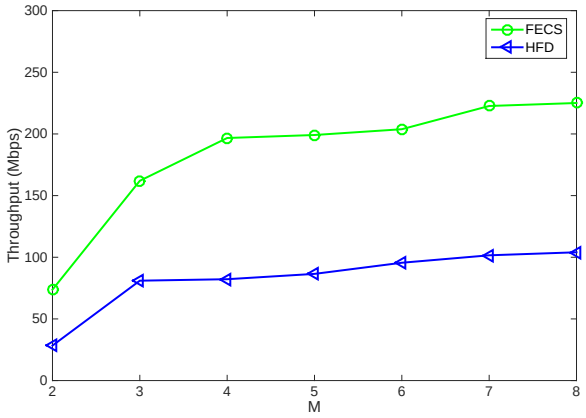

(b) Total network throughput.

Fig. 9. Throughput of two-node FD CSMA networks with different densities.

can not be prevented with carrier-sensing mechanism, no matter how small the P_{th} is.

5.2 Throughput of Two-node FD CSMA Networks

5.2.1 Square Network

We evaluate the network throughput of two-node FD CSMA networks with different link densities. In particular, we consider a square area ($D * D$) divided into M^2 sub-squares, where $D = 800m$. A two-node FD link-pair is located in the center of each sub-square. Fig. 9 (a) shows an example of two-node FD network with $M = 2$. The two nodes of each link are on the circle with a radius of $0.5d_{max}$ at the center of each sub-square. In particular, the two nodes are located at the intersections of the circle and an arbitrary line through the center of each sub-square. Thus, the link length is d_{max}. The carrier-sensing power thresholds are set as $-78.06dBm$ and $-72.81dBm$, which can eliminate the hidden nodes in HFD and FECS, respectively. We simulate 7 such networks with M increasing from 2 to 8, and obtain the total network throughput for each case, as shown in Fig. 9 (b).

From Fig. 9 (b), we can observe that compared with half-duplex transmission, the network throughput of FECS is increased by more than 100% for all the choices of M.

This article has been accepted for publication in a future issue of this journal, but has not been fully edited. Content may change prior to final publication. Citation information: DOI 10.1109/TMC.2019.2895034, IEEE Transactions on Mobile Computing

When $M = 4$, the network throughput improvement is more significant, which is more than 139%. The significant throughput gain is brought by two benefits of the two-node FD transmissions. First, with full-duplexing, the throughput of each link-pair is significantly improved. Second, under the hidden-node-free requirement, the carrier-sensing power threshold of FECS can be set much larger than the one in HFD. Therefore, the spatial reuse of the two-node FD CSMA networks is also significantly improved.

5.2.2 The Impact of Imperfect Self-interference (SI) Cancellation

We evaluate the impact of imperfect SI cancellation on the throughput of two-node FD networks. The network topology is given in Fig. 9 (a). We vary the SI suppression from $80dB$ to $110dB$. When the SI suppression is $110dB$, the residual SI is comparable to the background noise. The network throughputs are showed in Fig. 10. We can find that only when SI cancellation is $80dB$, can we observe a noticeable throughput reduction. The reason is that when the residual SI is large, as can be seen from equation (20), it requires a large semi-major axis of the interference ellipse to guarantee successful transmissions. Consequently, as can be seen from equations (18) and (19), the semi-major axis of the carrier-sensing ellipse is increased and the required carrier-sensing power threshold is decreased to guarantee the network free of hidden nodes according to Theorem 1. Furthermore, lowering the carrier-sensing power threshold reduces the network spatial reuse and throughput. In addition, Fig. 10 also shows when the SI cancellation is larger than $90dB$, the residual SI has little influence on the network throughput since the residual SI is too small to affect the carrier-sensing threshold and the spatial reuse.

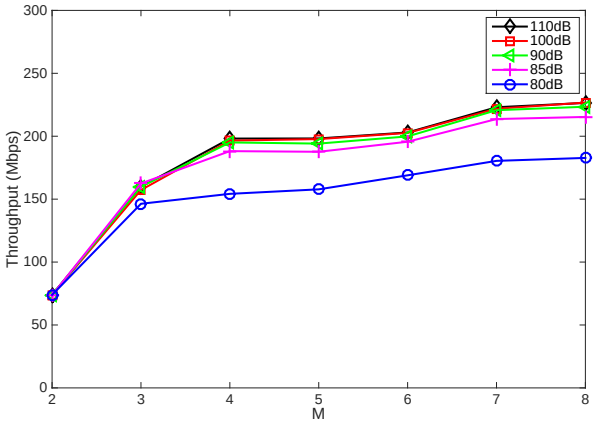

Fig. 10. Throughput of two-node FD network with different SI cancellation.

5.3 Throughput of Three-node FD CSMA Networks

We evaluate the network throughput of three-node FD CSMA networks with two different topologies, square network and chain network. In the following simulations, we assume that that self-interference is perfectly canceled, i.e., $I_{SI} = 0$.

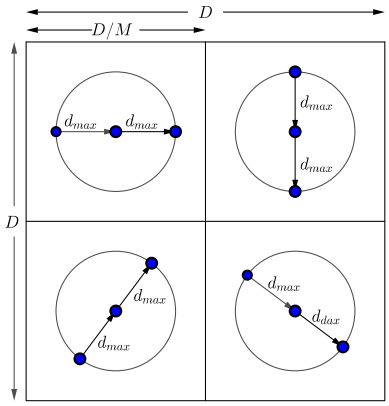

(a) Topology of a three-node FD network with $D = 1200m$ and $M = 2$.

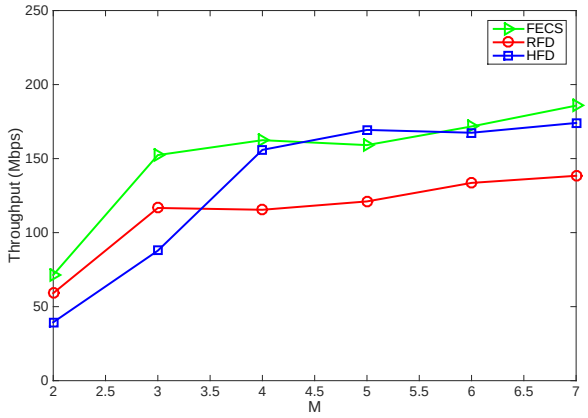

(b) Total network throughput.

Fig. 11. Throughput of three-node FD CSMA networks with different densities.

5.3.1 Square Network

We consider a $D * D$ square network with M^2 sub-squares. Fig.11 (a) shows a three-node FD CSMA network with $M = 2$. A three-node FD link-pair is located in the center of each sub-square. The FD relay node, which transmits and receives packet simultaneously, is placed at the center of each sub-square. The other two nodes are located on the circle with a radius of d_{max} centered in each sub-square. Specifically, they are located at the intersections of the circle and an arbitrary line through the center of each sub-squre. Thus, the link lengths of both the primary transmission and the secondary transmission are d_{max}. Notice that each three-node FD link-pair can be either source-based or destination-based depending on different initial transmission nodes. The link densities are changed by varying M from 2 to 7.

Fig. 11 (b) shows the network throughput of HFD, RFD and FECS. The carrier-sensing power thresholds are set as the values to prevent hidden-node collisions in each case. We can observe that our proposed FECS outperforms RFD for all the simulated networks. When $M = 7$, the network throughput is improved by more than 30%. The throughput improvement is brought by the secondary carrier-sensing design in our proposed FECS-MAC. With secondary carrier-sensing, the required P_{th} is increased, which improves the

This article has been accepted for publication in a future issue of this journal, but has not been fully edited. Content may change prior to final publication. Citation information: DOI 10.1109/TMC.2019.2895034, IEEE Transactions on Mobile Computing

network spatial reuse. We can further find that the network throughput of RFD is larger than the one in HFD only when $M = 2$ and $M = 3$. This is because that the three-node FD CSMA networks need a much smaller P_{th} than HD networks to prevent hidden-node collisions, which reduces the spatial reuse when the network becomes denser. Thus, although FD transmission may improve the transmission rate of each link-pair, the overall network throughput are even worse in dense networks. Although our proposed FECS improves the spatial reuse compared with RFD, the required P_{th} is still much smaller than the one in HD CSMA networks. Thus, the throughput improvement is still not significant for dense three-node FD CSMA networks.

5.3.2 Chain Network

We further investigate the throughput performance of a chain network shown in Fig. 12 (a). The nodes are placed on a straight line with separation equal to $50m$. Each node always has packets for the next one. Fig. 12 (b) shows the network throughput as the number of nodes in the chain is increased from 8 to 15. It is clear that our FECS outperforms other schemes. Using HFD as a baseline, we can observe that when the number of nodes in the chain is 15, RFD and our FECS can improve the network throughput by 24.1% and 47.5%, respectively. Compared with RFD, our FECS can further improve the average throughput by 19%. Such throughput gain is because of better spatial reuse in FECS.

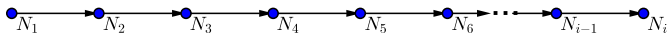

(a) Topology of a chain network.

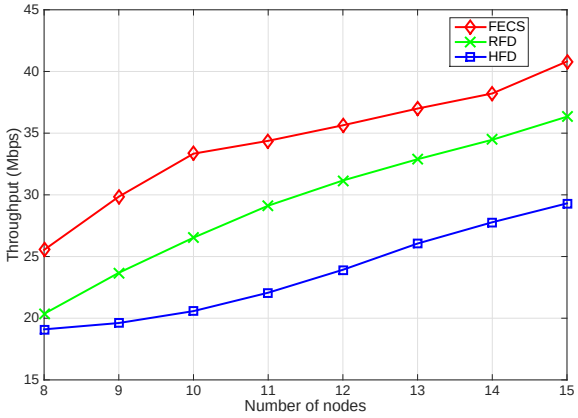

(b) Network throughput under HFD, RFD, and FECS.

Fig. 12. Network throughput of a chain network.

6 Conclusion

In this paper, we have given a comprehensive study on the hidden-node problem in FD CSMA networks. We first introduced the ellipse interference model and the ellipse carrier-sensing model to capture interference region and carrier-sensing region of a FD transmission link-pair, respectively. We further derived the sufficient condition on the carrier-sensing power threshold to eliminate the hidden nodes in FD CSMA networks. Such power requirement is much lower than the one needed in HD CSMA networks, which limits the spatial reuse. Therefore, we proposed the FECS-MAC protocol with the secondary carrier-sensing design to further improve the network spatial reuse while keeping the network free of hidden nodes.

There are a few research directions that need further studied. Both the theoretical studies and the simulation results have showed that the hidden-node problem in the three-node FD transmissions are a critical problem which may cause severe throughput degradation. Our FECS-MAC can improve the spatial reuse and the network throughput. However, in order to better exploit the full-duplex gain, especially in dense networks, we may need to consider more techniques such as the dynamic carrier-sensing and power control. Furthermore, the ellipse interference model proposed in this paper belongs to the pairwise interference model. It is interesting to consider the impact of cumulative interference from multiple currently active FD links. In this paper, we focused on the basic 802.11 random access mode. The RTS/CTS handshaking can alleviate the collisions in CSMA networks. However, the transmission cases that may cause hidden-node collisions in the RTS/CTS based protocols are more complicated. The hidden-node free design of the RTS/CTS based FD CSMA networks is an interesting yet challenging topic for future study.

References

[1] K. Tamaki, A. R. H., Y. Sugiyama, M. Bandai, S. Saruwatari, and T. Watanabe, "Full duplex media access control for wireless multi-hop networks," in *Proc. IEEE Veh. Technol. Conf.*, Jun. 2013.

[2] D. Bharadia, E. McMilin, and S. Katti, "Full duplex radios," in *Proc. ACM SIGCOMM*, vol. 43, no. 4, 2013.

[3] J. Mayank, C. J. Il, K. Taemin, B. Dinesh, S. Siddharth, S. Kannan, L. Philip, K. Sachin, and S. Prasun, "Practical, real-time, full duplex wireless," in *Proc. ACM MOBICOM*, 2011.

[4] C. J. Il, J. Mayank, S. Kannan, L. Phil, and K. Sachin, "Achieving single channel, full duplex wireless communication," in *Proc. ACM MOBICOM*, 2010.

[5] A. Sabharwal, P. Schniter, D. Guo, D. W. Bliss, S. Rangarajan, and R. Wichman, "In-band full-duplex wireless: Challenges and opportunities." *IEEE Jour. Select. Areas in Comm.*, vol. 32, no. 9, pp. 1637–1652, 2014.

[6] S. Goyal, P. Liu, O. Gurbuz, E. Erkip, and S. Panwar, "A distributed MAC protocol for full duplex radio," in *Proc. Asilomar Conf. on Sign., Syst. and Computers*, Nov. 2013.

[7] J. Y. Kim, O. Mashayekhi, H. Qu, M. Kazandjieva, and P. Levis, "Janus: A novel MAC protocol for full duplex radio," *Proc. CSTR*, vol. 2, no. 7, p. 23, 2013.

[8] K. Xu, M. Gerla, and S. Bae, "How effective is the IEEE 802.11 RTS/CTS handshake in ad hoc networks," in *Proc. IEEE GLOBECOM*, 2002.

[9] N. Singh, D. Gunawardena, A. Proutiere, B. Radunovi, H. V. Balan, and P. Key, "Efficient and fair MAC for wireless networks with self-interference cancellation," in *Proc. IEEE WiOpt*, May 2011.

[10] H. Ahn, G. Lee, and C. Kim, "Hidden chain: a full-duplex MAC protocol using hidden terminal relationships in WLANs," in *Proc. IEEE 12th Annual Conference on Wireless On-demand Network Systems and Services*, Jan. 2016.

[11] Y. Yang and N. B. Shroff, "Scheduling in wireless networks with full-duplex cut-through transmission," in *Proc. IEEE INFOCOM*, Apr. 2015.

[12] L. B. Jiang and S. C. Liew, "Improving throughput and fairness by reducing exposed and hidden nodes in 802.11 networks," *IEEE Trans. Mobile Comput.*, vol. 7, no. 1, pp. 34–49, Jan. 2008.

[13] L. Jiang and S. Liew, "Removing hidden nodes in IEEE 802.11 wireless networks," in *Proc. IEEE Veh. Technol. Conf.*, Sept. 2005.

[14] Z. J. Haas and J. Deng, "Dual busy tone multiple access (DBTMA)-a multiple access control scheme for ad hoc networks," *IEEE Trans. Commun.*, vol. 50, no. 6, pp. 975–985, Jun. 2002.
[15] Y. Zhang, L. Lazos, K. Chen, B. Hu, and S. Shivaramaiah, "FD-MMAC: Combating multi-channel hidden and exposed terminals using a single transceiver," in *Proc. IEEE INFOCOM*, Apr. 2014.
[16] K. M. Thilina, H. Tabassum, E. Hossain, and D. I. Kim, "Medium access control design for full duplex wireless systems: challenges and approaches," *IEEE Commun. Mag.*, vol. 53, no. 5, pp. 112–120, May 2015.
[17] R. Doost-Mohammady, M. Y. Naderi, and K. R. Chowdhury, "Performance analysis of CSMA/CA based medium access in full duplex wireless communications," *IEEE Trans. Mobile Comput.*, vol. 15, no. 6, pp. 1457–1470, 2016.
[18] W. Cheng, X. Zhang, and H. Zhang, "RTS/FCTS mechanism based full-duplex MAC protocol for wireless networks," in *Proc. IEEE GLOBECOM*, Dec. 2013.
[19] X. Xie and X. Zhang, "Does full-duplex double the capacity of wireless networks?" in *Proc. IEEE INFOCOM*, Apr. 2014.
[20] J. Hu, B. Di, T. Wang, K. Bian, and L. Song, "Hybrid MAC protocol for full duplex Wi-Fi networks," in *Proc. IEEE GLOBECOM*, Dec. 2017.
[21] L. Fu, S. C. Liew, and J. Huang, "Effective carrier sensing in CSMA networks under cumulative interference," in *Proc. IEEE INFOCOM*, Mar. 2010.
[22] I. C. S. L. M. S. Committee *et al.*, "Wireless LAN medium access control (MAC) and physical layer (PHY) specifications," *ANSI/IEEE Std. 802.11-1999*, 1999.
[23] A. Kochut, A. Vasan, A. U. Shankar, and A. Agrawala, "Sniffing out the correct physical layer capture model in 802.11b," in *Proc. 12th International Conference on Network Protocols*, Oct. 2004.
[24] L. B. Jiang and S. C. Liew, "Hidden-node removal and its application in cellular WiFi networks," *IEEE Trans. Veh. Technol.*, vol. 56, no. 5, pp. 2641–2654, 2007.
[25] Y. Yang, B. Chen, K. Srinivasan, and N. B. Shroff, "Characterizing the achievable throughput in wireless networks with two active RF chains," in *Proc. IEEE INFOCOM*, Apr. 2014.
[26] Z. Han, Y. Li, H. Tan, R. Wang, and Y. Zhang, "Cross-layer protocol design for wireless communication in hybrid data center networks," in *Proc. IEEE 12th MSN*, Dec. 2016.
[27] S. Chen, T. Huang, K. C. Lin, Y. W. P. Hong, and A. Sabharwal, "Probabilistic medium access control for full-duplex networks with half-duplex clients," *IEEE Trans. Wireless Commun.*, vol. 16, no. 4, pp. 2627–2640, 2017.
[28] ns3 Network Simulator, http://www.nsnam.org/.